Virology 405 (2010) 568–578

Contents lists available at ScienceDirect

Virology

journal homepage: www.elsevier.com/locate/yviro

Biochemical and genetic characterization of dengue virus methyltransferase

Hongping Dong [a,*], David C. Chang [a], Xuping Xie [a], Ying Xiu Toh [a,b], Ka Yan Chung [a,b], Gang Zou [a], Julien Lescar [b], Siew Pheng Lim [a], Pei-Yong Shi [a,*]

[a] Novartis Institute for Tropical Diseases, 10 Biopolis Road, #05-01 Chromos, Singapore 138670, Singapore
[b] School of Biological Sciences, Nanyang Technological University, 60, Nanyang Drive, Singapore 637551, Singapore

ARTICLE INFO

Article history:
Received 30 April 2010
Returned to author for revision
29 May 2010
Accepted 22 June 2010
Available online 23 July 2010

Keywords:
Dengue virus
Methyltransferase
RNA cap methylation
Flavivirus replication
Antiviral target

ABSTRACT

We report that dengue virus (DENV) methyltransferase sequentially methylates the guanine N-7 and ribose 2′-O positions of viral RNA cap (GpppA→m^7GpppA→m^7GpppAm). The order of two methylations is determined by the preference of 2′-O methylation for substrate m^7GpppA-RNA to GpppA-RNA, and the 2′-O methylation is not absolutely dependent on the prior N-7 methylation. A mutation that completely abolished the 2′-O methylation attenuated DENV replication in cell culture, whereas another mutation that abolished both methylations was lethal for viral replication, suggesting that N-7 methylation is more important than 2′-O methylation in viral replication. The latter mutant with lethal replication could be rescued by *trans* complementation using a wild-type DENV replicon. Furthermore, we found that chimeric DENVs containing the West Nile virus methyltransferase, polymerase, or full-length NS5 were nonreplicative, but the replication defect could also be rescued through *trans* complementation using the wild-type DENV replicon.

Introduction

Dengue virus (DENV) is a mosquito-borne emerging or reemerging pathogen. There are four distinct serotypes of DENV that infect humans, causing diseases ranging from acute self-limiting febrile illness to life-threatening dengue hemorrhagic fever (DHF) and dengue shock syndrome (DSS). More than 2 billion people in tropical and subtropical regions are at risk of DENV infection, leading to 50 to 100 million human infections and 24,000 deaths each year. Neither vaccine nor antiviral therapy is currently available for prevention and treatment of DENV infections. Besides DENV, many other flaviviruses, including West Nile virus (WNV), yellow fever virus (YFV), Japanese encephalitis virus (JEV), and tick-borne encephalitis (TBEV), also cause significant human mortality and morbidity (Gubler et al., 2007).

DENV belongs to genus flavivirus in family *Flaviviridae*. The flavivirus genome is a single, positive-strand RNA of approximately 11 kb in length. It consists of a 5′-untranslated region (UTR), a long open reading frame (ORF), and a 3′-UTR. The ORF encodes a polyprotein that is post- and cotranslationally cleaved by viral and cellular proteases to three structural proteins (capsid [C], premembrane [prM]/membrane [M], and envelope [E]) and seven nonstructural proteins (NS1, NS2a, NS2b, NS3, NS4a, NS4b, and NS5) (Lindenbach et al., 2007). The 5′ end of the genomic RNA contains a type 1 cap structure (m^7GpppAm) (Cleaves and Dubin, 1979; Wengler, 1981), which is similar to the cap structure of most eukaryotic and viral mRNAs. The cap structure is known to be critical for mRNA stability and efficient translation (Furuichi and Shatkin, 2000).

RNA cap formation generally requires four enzymatic reactions (Shuman, 2001). First, the 5′-triphosphate end of nascent RNA transcript is hydrolyzed to a 5′-diphosphate by an RNA triphosphatase. Second, the 5′-diphosphate RNA is capped with GMP (using GTP) by an RNA guanylyltransferase. Third, the N-7 position of guanine cap is methylated by an RNA guanine-methyltransferase (N-7 MTase). Lastly, the first and second nucleotides of many cellular and viral mRNAs are further methylated at the ribose 2′-OH position by a nucleoside 2′-O MTase, resulting in cap 1 (m^7GpppNm) and cap 2 (m^7GpppNmNm) structures, respectively. *S*-adenosyl-L-methionine (SAM) is the methyl donor for both N-7 and 2′-O methylations. After each methylation event, SAM is converted to the by-product *S*-adenosyl-L-homocysteine (SAH). For flavivirus RNA cap formation, the RNA triphosphatase has been mapped to NS3 (Li et al., 1999; Wengler and Wengler, 1991); the N-7 and 2′-O MTase activities have been located to the N-terminal region of NS5 (Egloff et al., 2002; Ray et al., 2006; Zhou et al., 2007); recent studies suggest that the guanylyltransferase may also reside in the MTase domain of NS5 (Egloff et al., 2007; Issur et al., 2009).

The current understanding of flavivirus RNA cap methylation has been mainly derived from WNV MTase. The WNV MTase domain was shown to catalyze N-7 and 2′-O methylations in a sequential manner, with N-7 preceding 2′-O methylation (Zhou et al., 2007). Unlike cellular RNA cap methyltransferase, WNV MTase requires specific viral RNA sequence and structure for its methylation reactions (Dong et al., 2007). Structure-based mutagenesis studies suggest that the

* Corresponding authors. Fax: +65 67222916.
E-mail addresses: hongping.dong@novartis.com (H. Dong), pei_yong.shi@novartis.com (P.-Y. Shi).

0042-6822/$ – see front matter © 2010 Elsevier Inc. All rights reserved.
doi:10.1016/j.virol.2010.06.039

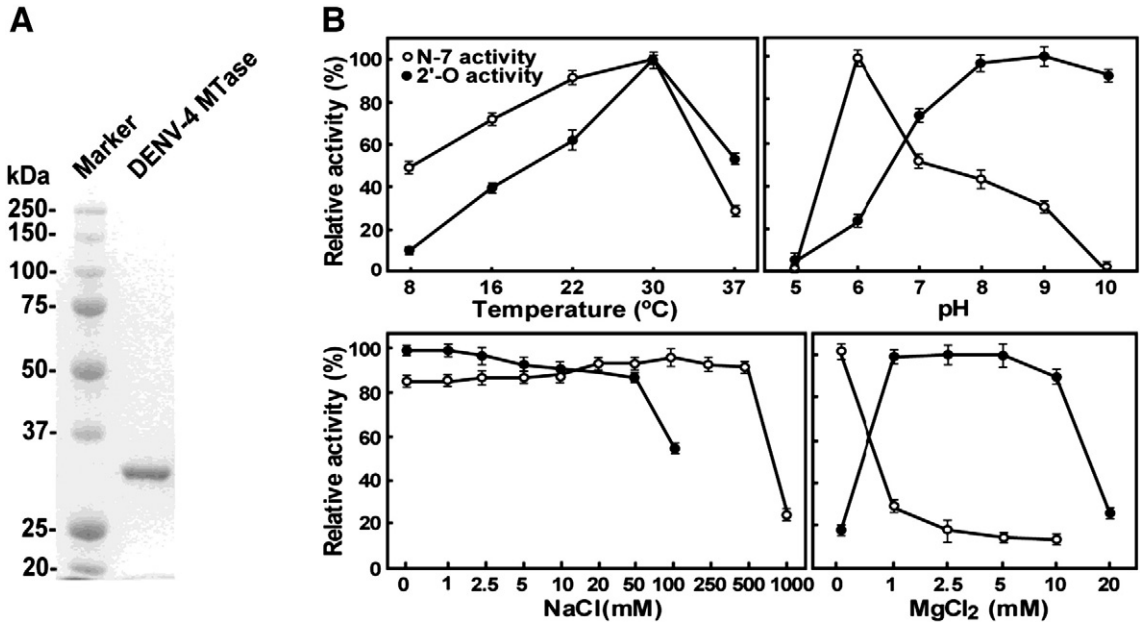

Fig. 1. Optimal conditions for N-7 and 2′-O cap methylations of DENV-4 MTase. (A) SDS-PAGE analysis of recombinant DENV-4 MTase. Molecular masses of protein markers are labeled. (B) Optimal conditions for N-7 and 2′-O cap methylations. The N-7 and 2′-O methylation assays were performed using substrate G*pppA-RNA and m^7G*pppA-RNA, respectively; the reactions were incubated for 5 min for N-7 methylation and 60 min for 2′-O methylation. The reaction mixtures were digested with nuclease P1 and analyzed on TLC plates. The products on TLC plates were quantified by PhosphorImager analysis. Optimal temperature, pH, NaCl concentration, and $MgCl_2$ concentration were obtained by titrating individual parameter while keeping other parameters at the optimal levels. Relative methylation activities are presented using the optimal level as 100%. Average results from three independent experiments are shown.

WNV MTase catalyzes the two methylation events through an RNA substrate repositioning model (Dong et al., 2008a; Dong et al., 2008b). Experiments using a luciferase-reporting replicon and an infectious clone of WNV showed that the N-7 methylation is critical for efficient RNA translation as well as for viral replication. In contrast, mutations that completely destroyed 2′-O methylation attenuated WNV replication in cell culture and in mice (Zhou et al., 2007). Furthermore, WNV MTase was found to genetically interact with the RNA-dependent RNA polymerase (RdRp) domain of NS5 as well as the 5′ stem-loop of genomic RNA (Zhang et al., 2008). The WNV results suggest that flavivirus MTase represents a new antiviral target (Dong et al., 2008c). However, it remains to be experimentally demonstrated whether the conclusions derived from the WNV MTase are applicable to other members of the flavivirus genus. A systematic analysis of MTase from other flaviviruses is required to generalize the mechanism for flavivirus cap methylations.

Our long-term goal is to develop small-molecule inhibitor for clinical treatment of DENV infection. To examine whether MTase is a valid target for anti-DENV drug discovery, we performed biochemical and genetic characterizations of the DENV MTase. Our results demonstrate that MTases from DENV and WNV share a common mechanism in catalyzing the two cap methylation reactions. Importantly, mutagenesis experiments using an infectious cDNA clone of DENV suggest that N-7 methylation, rather than 2′-O methylation, is critical for DENV replication. These results have established a foundation to target N-7 methylation for DENV drug discovery.

Results

Distinct conditions required for DENV N-7 and 2′-O methylations

We cloned, expressed, and purified the MTase domain, representing the N-terminal 272 amino acids of DENV-4 NS5. An SDS–PAGE analysis showed that the protein was >90% pure with an expected molecular mass of 30 kDa (Fig. 1A). The recombinant MTase was used to search for optimal assay conditions for methylation reactions (Fig. 1B). To avoid artifacts, we used an authentic RNA substrate,

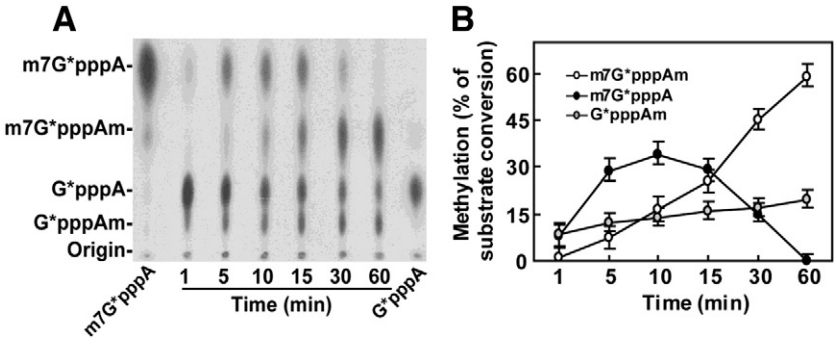

Fig. 2. Time course analysis of DENV MTase activities. ^{33}P-labeled G*pppA-RNA (representing the first 211 nucleotides of DENV genome) was incubated with DENV-4 MTase in 2′-O buffer (pH 9.0). The reactions were terminated at indicated time points, digested with nuclease P1, analyzed on a TLC plate (A), and quantified using a PhosphorImager. For each time point, the relative conversions of G*pppA to m^7G*pppA, m^7G*pppAm, and G*pppAm are presented (B). The input G*pppA-RNA at 0 min was set at 100%. The positions of the origin and the migrations of G*pppA, m^7G*pppA, m^7G*pppAm, and G*pppAm molecules are indicated on the left side of the TLC image. The mobility of G*pppAm on TLC was assigned according to the VP39-mediated reaction (see details in Fig. 4A).

representing the 5′-terminal 211 nucleotides (nt) of the DENV genome. The N-7 methylation was monitored by the conversion of G*pppA-RNA to m^7G*pppA-RNA (the symbol * indicates that the following phosphate is ^{33}P-labeled). The 2′-O methylation was measured by the conversion of m^7G*pppA-RNA to m^7G*pppAm-RNA. The reactions were digested by nuclease P1 to release G*pppA, m^7G*pppA, and m^7G*pppAm, which were separated on a TLC plate. Using these methods, we varied several parameters and quantified

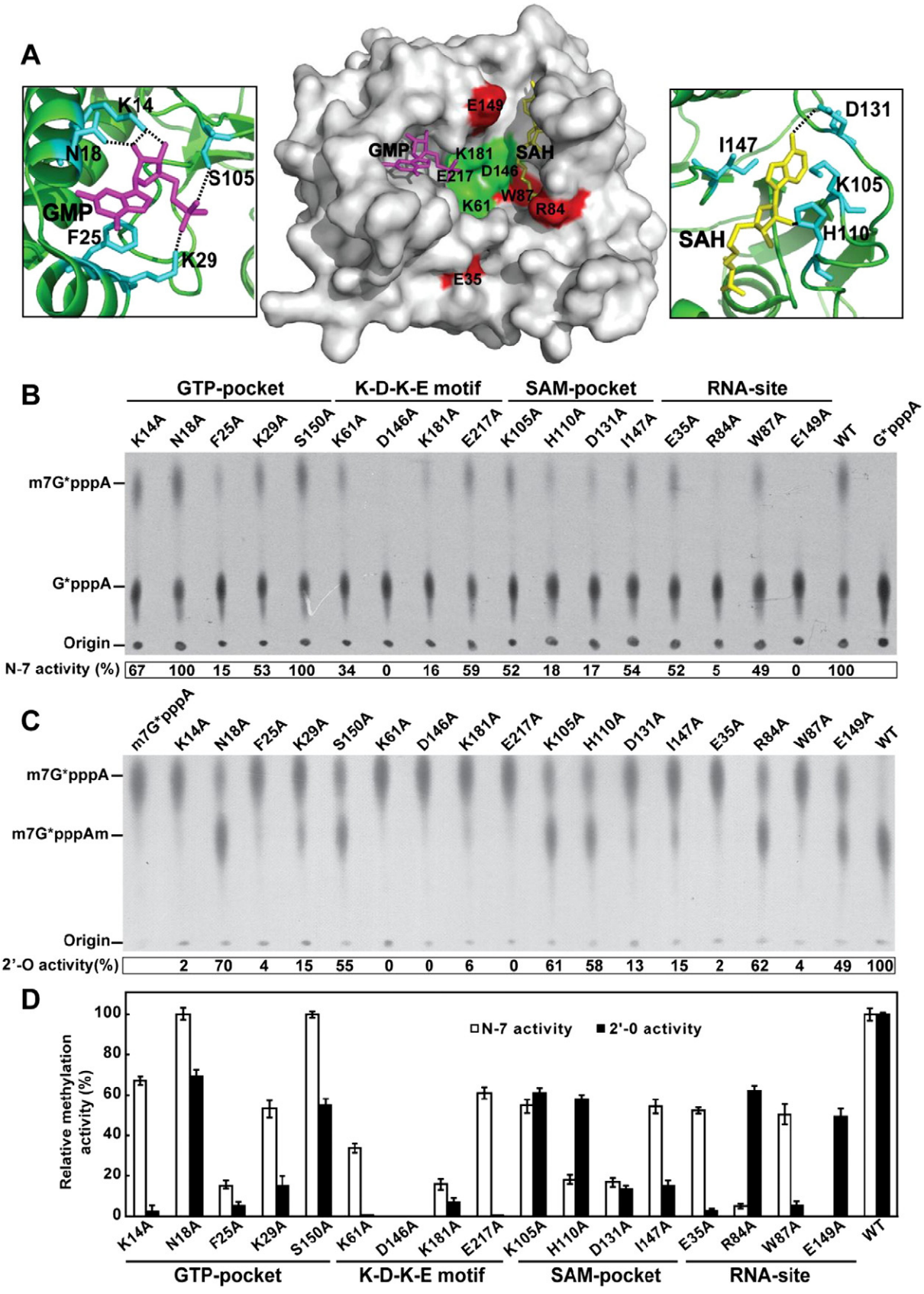

their effects on methylation efficiency. As plotted in Fig. 1B, both N-7 and 2′-O methylations shared a same optimal temperature at 30 °C. However, the two methylations require different pH, and NaCl and $MgCl_2$ concentrations. The optimal pH for N-7 and 2′-O methylation were at 6.0 and 8.0–10.0, respectively. Concentrations of NaCl at >500 mM and >50 mM inhibited N-7 and 2′-O methylation, respectively. The presence of $MgCl_2$ inhibited N-7 methylation, whereas $MgCl_2$ concentration at 1–5 mM exhibited optimal 2′-O methylation. These results demonstrate that distinct conditions are required for DENV-4 N-7 and 2′-O methylations.

Order of N-7 and 2′-O methylations of viral RNA cap

A time course of methylation was performed to examine the order of N-7 and 2′-O methylations. G*pppA-RNA was incubated with DENV-4 MTase in a reaction buffer at pH 9.0, which supports both methylation activities (as shown in Fig. 1B). The reaction was terminated at various time points and assayed on a TLC plate. As shown in Fig. 2, m^7G*pppA was observed as early as 1 min, saturated at 5–15 min, and steadily declined at later time points. Concurrently, m^7G*pppAm product was first detected at 5 min and increased up to 60 min. These results suggest that DENV-4 MTase catalyzes the two methylations in an order of GpppA→m^7GpppA→m^7GpppAm. Meanwhile, a consistent level of G*pppAm (determination of G*pppAm mobility on TLC plates is described in detail in Fig. 4A) was observed throughout the experiment, indicating that 2′-O methylation is not absolutely dependent on the prior N-7 methylation.

Distinct amino acid requirements for the N-7 and 2′-O methylations

Flavivirus MTase has a conserved structure with a SAM-binding pocket, a GTP-binding pocket, a RNA-binding site, and a K-D-K-E motif (Egloff et al., 2002; Zhou et al., 2007). The K-D-K-E motif forms the active site that is conserved among 2′-O MTases from various organisms (Egloff et al., 2002; Hager et al., 2002; Hodel et al., 1996). Using the crystal structure of DENV-2 MTase as a guide (Egloff et al., 2002), we performed a systematic mutagenesis of the DENV-4 MTase. For every structural pocket or motif, a panel of mutant MTases, each of which contained an Ala substitution of one amino acid, were prepared and assayed for cap methylations.

K-D-K-E motif

The K-D-K-E motif is well known to catalyze an S_N2-reaction mediated 2′-O methyl transfer (Hodel et al., 1996). In DENV MTase, this motif is formed by K61-D146-K181-E217 (Fig. 3A, middle panel, green). Methylation assays showed that K61A, D146A, and E217A MTases mutants were completely inactive in 2′-O methylation, while the K181A mutant retained 6% 2′-O activity of the WT enzyme (Fig. 3C). For N-7 methylation, only the D146A mutant completely lost the N-7 activity; the K61A, K181A, and E217A mutants retained 34%, 16%, and 59% of the WT activity, respectively (Fig. 3B). The results demonstrate that residues K61, D146, and E217 of the K-D-K-E motif are essential for the 2′-O methylation, whereas only D146 is essential for the N-7 activity.

SAM-binding pocket

Four residues within the SAM-binding pocket were selected for mutagenesis analysis, among which K105 and I147 sandwich the adenosine base, D131 interacts with the amide of the adenosine, and H110 forms a hydrogen bond with the 2′-OH of the ribose (Fig. 3A, right panel, residues in cyan). Methylation assays showed that substitutions of K105, H110, D131, and I147 with Ala affected both the N-7 and 2′-O methylations (Figs. 3B and 4C), suggesting that the single SAM-binding site is responsible for both methylations. Since the SAM molecule is bound to the SAM pocket through interactions with multiples residues, a single point mutation is not sufficient to completely abolish the methylation activities.

GTP-binding site

For the GTP-binding pocket, five residues were individually substituted with Ala. F25 stacks with the guanine base; K14 interacts with the 2′-OH and 3′-OH of the ribose; N18 forms a hydrogen bond with the 2′-OH of the ribose; and K29 and S150 interact with the α-phosphate of GTP (Fig. 3A, left panel, cyan). Methylation assays showed that only F25A significantly decreased the N-7 methylation, with 15% of the WT level; substitutions of other residues exhibited minor effects on N-7 methylation, with 53–100% of the WT activity (Fig. 3B). For 2′-O methylation, K14A, N18A, and K29A reduced the activity by ≥85%; N18A and S150A suppressed 30% and 45% of the 2′-O activity, respectively. These results suggest that the GTP-binding pocket selectively functions during 2′-O methylation.

RNA-binding site

To identify critical residues within the putative RNA-binding site, we selected four residues on enzyme surface for Ala-scanning mutagenesis (Fig. 3A, middle panel, residues in red). The E35A and W87A substitutions reduced N-7 methylation to about 50% of the WT level (Fig. 3B), but almost completely abolished 2′-O methylation, with ≤4% of the WT activity (Fig. 3C). In contrast, the R84A and E149A mutations were selectively important for N-7 methylation, with ≤5% of the WT activity (Fig. 3B), while retained 49–62% of the WT 2′-O activity (Fig. 3C). Based on the above mutagenesis results (Fig. 3D), we conclude that distinct residues are required for the two methylation events.

2′-O methylation prefers a substrate with prior N-7 methylation

We asked what factor determines the order of GpppA→m^7GpppA→m^7GpppAm, as observed in Fig. 2. The E149A mutant was selected to address this question as it was completely inactive in N-7 methylation while retaining 49% of WT 2′-O methylation (Fig. 3D). A time course experiment was performed using E149A and substrate G*pppA-RNA or m^7G*pppA-RNA in the 2′-O assay buffer (pH 9.0). After nuclease P1 digestion, the reactions were resolved on TLC plates (Fig. 4A) and 20% polyacrylamide denaturing gels (Fig. 4B). The denaturing gel was used as an alternative means to separate G*pppA, G*pppAm, m^7G*pppA, and m^7G*pppAm, as previously reported (Dong et al., 2008a). Vaccinia protein 39 (VP39), a well-known 2′-O MTase, was included as the positive control. As shown in Fig. 4A, the mobility

Fig. 3. Mutagenesis analysis of DENV-4 MTase. (A) Surface representation of DENV-2 MTase in complex with GMP and SAH (middle panel). GMP (magenta) and SAH (yellow) molecules are shown in stick presentation. Residues forming the K-D-K-E tetrad are shown in green. Residues mutated within the putative RNA-binding site are in red. Left panel: Five residues (cyan) forming direct interactions with GMP molecule in the GTP-binding pocket. Hydrogen bonds are indicated by dashed black lines. Right panel: Four residues (cyan) interacting with the adenosine moiety of the SAH molecule. The images were produced using DENV-2 MTase structure (PDB code: 1L9K; Egloff et al., 2002) and PyMOL. (B) Effects of mutations within the K-D-K-E tetrad, SAM-, GTP-, and putative RNA-binding sites on DENV-4 N-7 methylation. Substrate G*pppA-RNA, representing the first 211 nucleotides of the DENV genome, was incubated with WT or various mutant MTases at room temperature for 5 min in the presence of SAM. The reaction mixtures were digested with nuclease P1, analyzed on a TLC plate, and quantified using a PhosphorImager. The methylation efficiencies of mutant MTases were compared with that of the WT MTase (set at 100%), and these are indicated below the TLC image. The MTase variants are labeled at the top of the TLC autoradiograph. (C) Effects of mutations on DENV 2′-O methylation. The experiments were performed as described in (B), except that substrate m^7G*pppA-RNA was incubated in 2′-O buffer (pH 9.0). The conversion of m^7G*pppA-RNA→m^7G*pppAm-RNA was quantified using a PhosphorImager. ^{33}P-labeled markers (G*pppA and m^7G*pppA) are indicated at the top of TLC images. The position of the origin and the migration positions of the G*pppA, m^7G*pppA, and m^7G*pppAm molecules are shown to the left of the TLC images. (D) Summary of methylation results from panels B and C. Averages of three independent experiments are presented.

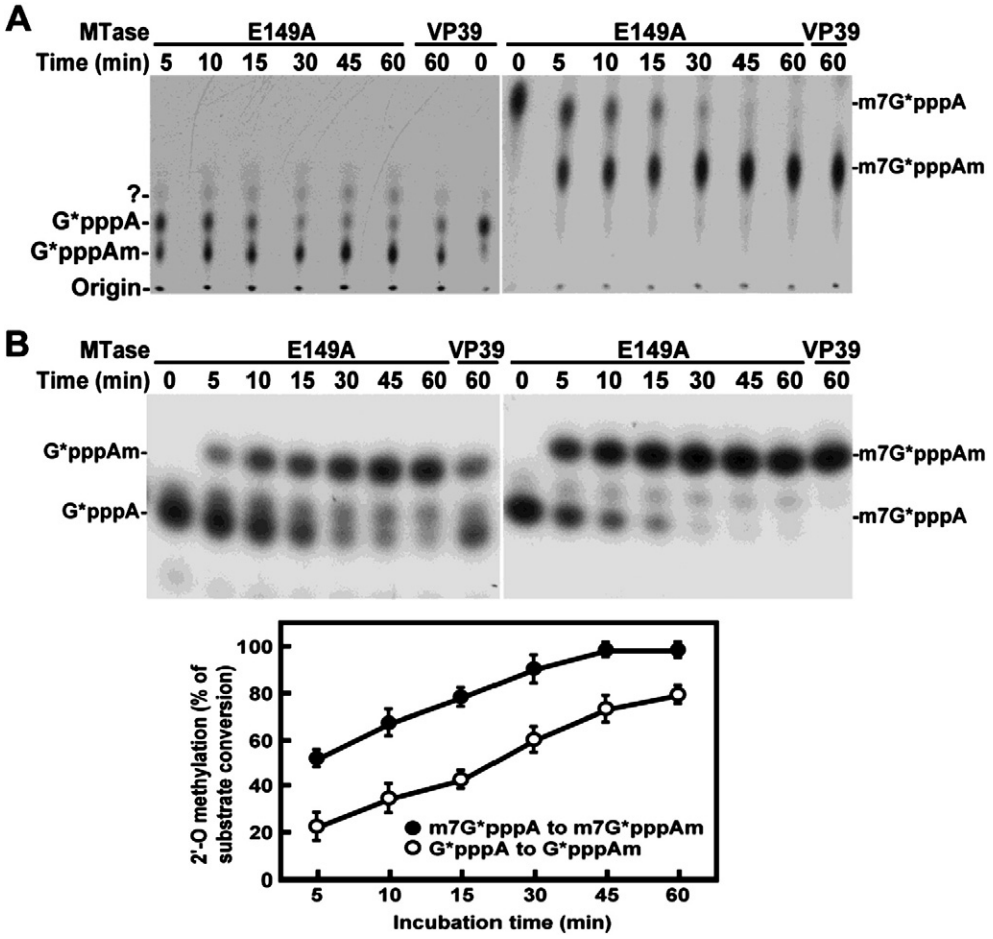

Fig. 4. Analysis of 2′-O methylation using E149A MTase. E149A MTase was incubated with m^7G*pppA-RNA (A) and G*pppA-RNA (B) in 2′-O buffer (pH 9.0). The reactions were terminated at different time points, subjected to nuclease P1 digestion, and analyzed on TLC plates (A) and on a 20% denaturing polyacrylamide gel containing 8 M urea (B). VP39, a known 2′-O MTase, was included as a positive control. The enzyme, RNA substrate, and reaction time are indicated. The positions of G*pppA, m^7G*pppA, G*pppAm, and m^7G*pppAm molecules are labeled to the left of the TLC plates and gels. The bottom panel in (B) summarizes the conversions of GpppA-RNA→GpppAm-RNA and m^7GpppA-RNA→m^7GpppAm-RNA that were quantified using PhosphorImager. Conversion percentage = product / (residual substrate + product) × 100%. See details in Materials and methods.

of G*pppAm on TLC was assigned according to the VP39-mediated reaction; a weak band of unknown identity (labeled with "?") was also observed in all reactions. Nevertheless, the TLC (Fig. 4A) and denaturing gel analyses (Fig. 4B) showed that E149A could perform 2′-O methylation on both m^7G*pppA-RNA and G*pppA-RNA. However, the conversion of m^7G*pppA-RNA→m^7G*pppAm-RNA was more efficient than the G*pppA-RNA→G*pppAm-RNA conversion (Fig. 4B, bottom panel). The results suggest that a substrate with prior N-7 methylation is preferred for the 2′-O methylation; this substrate preference determines the dominant methylation order of GpppA→m^7GpppA→m^7GpppAm. It is of note that the flavivirus mRNA cap methylation shows that m^7GpppAm has a lower Rf (retardation factor) than m^7GpppA, which is the opposite of what should occur.

Effect of MTase on DENV replication

To analyze the biological relevance of MTase, we performed mutagenesis analysis using a DENV-1 infectious cDNA clone. Based on the above biochemical results, two mutations were selected for viral replication analysis (Fig. 5). E217A which was completely defective in 2′-O methylation, but retained 59% of N-7 methylation activity, and D146A was completely inactive in both methylations. Three parameters were used to monitor the effect on viral replication. Firstly, after electroporation of BHK-21 cells with equal amounts of WT and mutant genome-length RNAs, immunofluorescence assay (IFA) was performed to detect viral E protein expression. As shown in Fig. 5A, transfection of WT RNA generated IFA-positive cells on day 1 posttransfection (p.t.), and the number of positive cells increased from day 1 to 4. Transfection of E217A RNA also generated IFA-positive cells, but the number of positive cell was fewer compared to WT. In contrast, no E-positive cells were observed in BHK-21 cells transfected with D146A RNA even on day 5 p.t. (Fig. 5A). Secondly, plaque assays showed that cells transfected with the WT and E217A RNAs generated viruses; the E217A virus produced smaller plaques than the WT virus (Fig. 5B). Sequencing of the complete NS5 gene of E217A virus confirmed that the engineered nucleotides were retained with no other mutations (data not shown). Plaque assay using supernatant from cells transfected with the D146A RNA did not generate plaques (Fig. 5B); continuous passaging of the D146A RNA-derived culture fluids on naive cells did not yield viruses that could be detected by plaque assays or RT–PCR (data not shown). Thirdly, growth kinetics were compared between the WT and E217A viruses on Vero and mosquito C6/36 cells. The E217A virus grew slightly slower (<4-fold in viral titer) than the WT virus on Vero cells (Fig. 5C, left panel). The growth difference on C6/36 cells was more dramatic (10- to 50-fold in viral titer) between the WT and E217A viruses. These results indicate that a mutation defective in 2′-O methylation does not significantly affect DENV replication, whereas a mutation defective in N-7 methylation could be lethal for DENV replication.

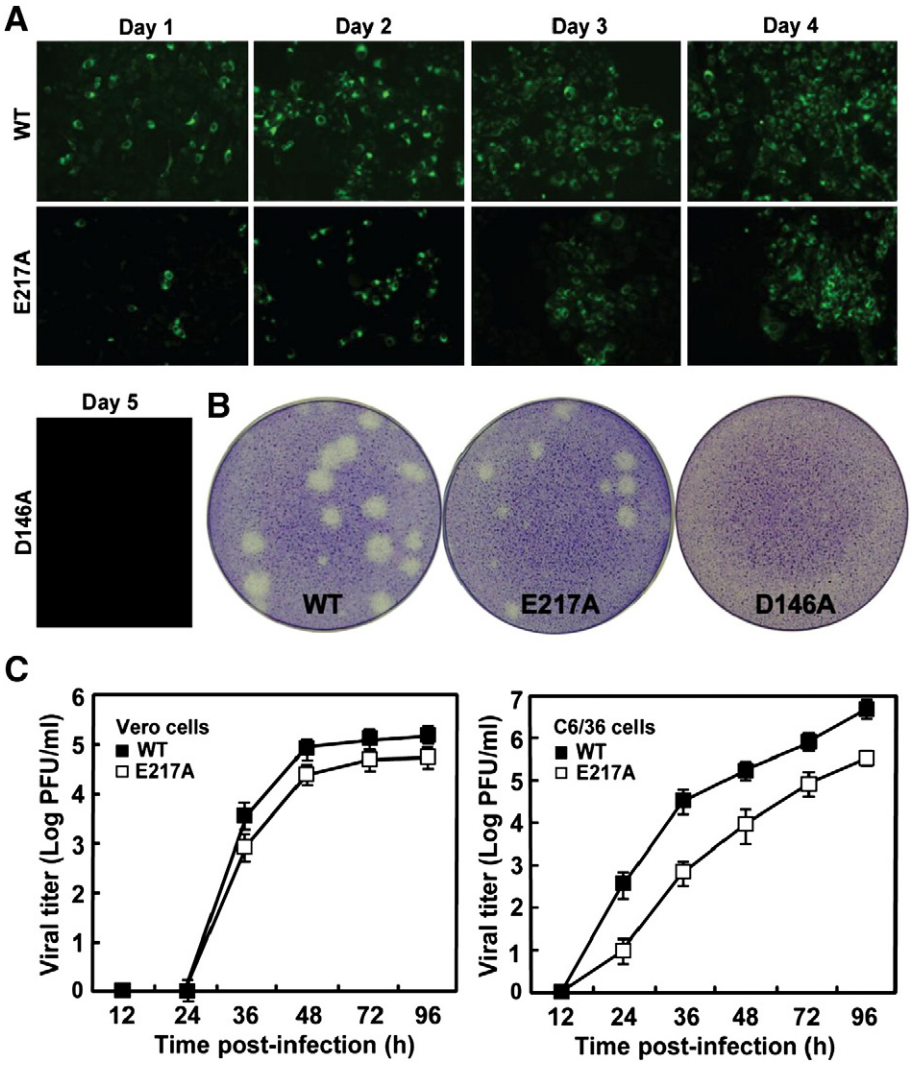

Fig. 5. Mutagenesis of MTase in the context of DENV replication. (A) IFA analysis. BHK-21 cells were electroporated with WT and mutant (D146A and E217A) genome-length RNAs. The transfected cells were subjected to IFA analysis using mouse monoclonal antibody 4G2 (against DENV E protein) and anti-mouse immunoglobulin G conjugated with FITC as the primary and secondary antibodies, respectively. Similar number of cells was observed for all images under phase contrast (data not shown). (B) Plaque morphology of WT and E217A mutant viruses. No plaques could be detected for cells transfected with the D146A genome-length RNA. (C) Growth kinetics of WT and mutant E217A viruses. Vero and C6/36 cells were infected with the WT and E217A viruses at an MOI of 0.2. Supernatants of the infected cells were collected at different time points and assayed for viral titers using plaque assay.

trans-Complementation of lethal MTase mutation

Since the D146A mutation is lethal for viral replication, we asked whether the replication defect could be overcome by *trans* complementation. A DENV-1 genome-length RNA containing the D146A mutation was transfected into BHK-21 cells harboring a DENV-1 replicon. The transfected cells were examined for viral E protein expression with IFA. Since the replicon lacks E gene, the detection of E protein-positive cells could indicate the replication of the transfected genome-length RNA. Upon transfection with the D146A genome-length RNA, E protein-positive cells were clearly observed in the replicon-containing cells, but no IFA-positive cells were detected in the transfected cells without replicon (Fig. 6A). As a positive control, WT genome-length RNA was transfected into both naive BHK-21 cells and the replicon-carrying cells; both cells produced E protein-positive cells. Interestingly, WT RNA produced more IFA positive foci in the naive cells than those in the replicon-containing cells; this phenomenon could be due to superinfection exclusion, as recently reported for WNV (Zou et al., 2009).

To exclude the possibility that the replication of D146A RNA in the replicon-containing cells was due to a reversion, a second site adaptation, or a recombination between the replicon and mutant genome-length RNA, we passaged the culture fluids from the RNA-transfected cells (with replicon) on naive Vero cells (without replicon) for three rounds. The Vero cells were examined for E protein expression using IFA. If reversion or recombination has had occurred, the cells would have become E-positive due to the replication of the reverted genome-length RNA. On the contrary, no E-positive cells were detected during the culture fluid passaging (data not shown), indicating that revertant or recombinant viruses had not emerged from the D146A mutant.

We also performed RT–PCR to confirm the *trans* complementation results. On day 4 post-transfection, total cellular RNA and culture fluid RNA were extracted. The extracted RNAs were subjected to RT–PCR using primers targeting viral structural prM and E genes; these primers could only amplify genome-length RNA, not replicon RNA (due to absence of structural genes). As shown in Fig. 6B, no RT–PCR product was detected from BHK-21 cells transfected with mutant D146A RNA (lane 3). In contrast, the D146A RNA was readily detected by RT–PCR (862-bp product) in transfected replicon-containing cells (Lane 1) and supernatant (Lane 2). As a positive control, supernatant RNA derived from the cells transfected with WT RNA yielded RT–PCR product (lane 4). Overall, the IFA and RT–PCR results demonstrate that the replication defect of an inactive MTase for both methylation types could be rescued by *trans* complementation in DENV.

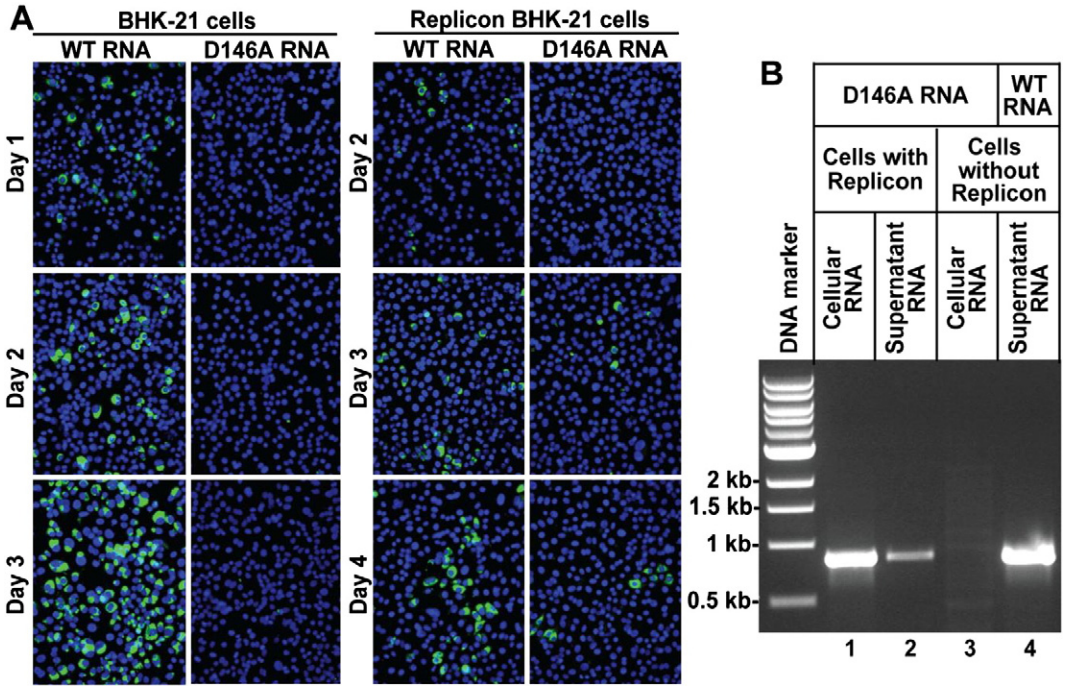

Fig. 6. *trans* complementation of mutant D146A genome-length RNA. (A) IFA analysis. WT and D146A genome-length RNAs (2 μg) were transfected into naive BHK-21 cells with or without a DENV-1 replicon. IFA was performed to detect viral E protein expression (stained in green) in the transfecetd cells at indicated time points. Nuclei were counter stained with DAPI in blue. (B) RT–PCR analysis. On day 4 post-transfection, RNA was extracted from cells and supernatants, and subjected to RT–PCR amplification using primers targeting viral prM and E genes. The RT–PCR products were analyzed on a 1% agarose gel. Various experimental conditions are indicated above the image of agarose gel. See experimental details in Materials and methods.

trans-Complementation of chimeric DENV-2 containing WNV MTase, RdRp, or full-length NS5

Since the above D146A point mutant represents the first success of *trans* complementation of flavivirus MTase, we asked whether other types of mutations within MTase, RdRp, or both domains could be *trans* complemented. To address this question, we generated a panel of chimeric DENV-2, in which the DENV MTase domain, RdRp domain, or full-length NS5 gene was individually substituted with the WNV counterparts, resulting in DENV-2 $MTase_{WNV}$, DENV-2 $RdRp_{WNV}$, and DENV-2 $NS5_{WNV}$, respectively (Fig. 7A). Upon transfection of the genome-length RNAs into naive BHK-21 cells, only the DENV-2 WT RNA produced E-positive cells; none of the chimeric RNAs generated E-positive cells (Fig. 7B), indicating that the chimeric RNAs are nonreplicative. In contrast, after transfection of the genome-length RNAs into BHK-21 cells containing DENV-2 replicon, all three chimeric RNAs generated E-positive cells, although the number of E-positive cells was fewer than that generated by the DENV-2 WT RNA. These results confirmed that the replication defect of NS5 (MTase and/or RdRp) could be rescued by *trans* complementation in DENV. Continuous passaging of the supernatants on naive BHK-21 cells or on replicon-containing BHK-21 cells did not yield viruses that could replicate on BHK-21 cells without replicon (data not shown).

Discussion

We characterized various aspects of the DENV MTase using both biochemical and genetic approaches. Assay optimization showed that DENV MTase requires distinct biochemical conditions for N-7 and 2′-O methylations (Fig. 1B). The high pH requirement for the 2′-O methylation supports the S_N2 mechanism of methyl transfer (Hager et al., 2002; Hodel et al., 1998). It was proposed that high pH facilitates the K-D-K-E motif-mediated deprotonation of the target 2′-OH, which nucleophilically attacks the methyl moiety of SAM for methyl transfer (Zhou et al., 2007). The requirement of high pH for methylation was also reported for DIM-5, a histone H3 lysine 9 MTase (Zhang et al., 2002). However, the question remains as to how the MTase overcomes the requirement of high pH during replication inside cells. One speculation is that the local p*K*a of Lys within the K-D-K-E motif is lowered in the membrane-associated replication complex; alternatively, interactions with other viral or cellular proteins may lower the pH dependence of the MTase reaction.

The conversion of GpppA-RNA→m^7GpppA-RNA→m^7GpppAm-RNA was evident in a time course experiment (Fig. 2). The order of two methylations is similar to that of host mRNA cap methylation events (Shuman, 2001). However, the exact sequence of methylations in the context of flavivirus replication remains to be experimentally demonstrated. Nevertheless, like WNV MTase, the DENV MTase uses a single SAM-binding site to donate methyl groups to both N-7 and 2′-O positions of viral RNA cap in a sequential manner. Two potential mechanisms could underlie this sequential outcome: The 2′-O activity is absolutely dependent on the prior N-7 methylation; alternatively, the 2′-O methylation is more efficient when using an m^7GpppA-RNA substrate compared with a GpppA-RNA substrate. Using a 2′-O-active, but N-7-defective mutant MTase (E149A), we showed that E149A could catalyze the conversions of both m^7GpppA-RNA→m^7GpppAm-RNA and GpppA-RNA→GpppAm-RNA (Fig. 4). The conversion of GpppA-RNA→GpppAm-RNA demonstrates that the 2′-O methylation is not absolutely dependent on the N-7 methylation (Figs. 2 and 4). The independence of 2′-O methylation on N-7 methylation was also shown in other DENV studies (Egloff et al., 2002; Lim et al., 2008). However, the current study showed that the efficiency of m^7GpppA-RNA→m^7GpppAm-RNA was more efficient than that of GpppA-RNA→GpppAm-RNA. The latter result is in disagreement with a recent DENV MTase study which showed the efficiency of 2′-O methylation was similar when using either m^7GpppACn or GpppACn as substrates (Selisko et al., 2010). The discrepancy could have been caused by different RNA substrates: An authentic viral RNA was used in this study, whereas the other study used a short nonviral RNA. The difference in RNA substrate could also explain the lack of detection of N-7 methylation when the nonviral RNA

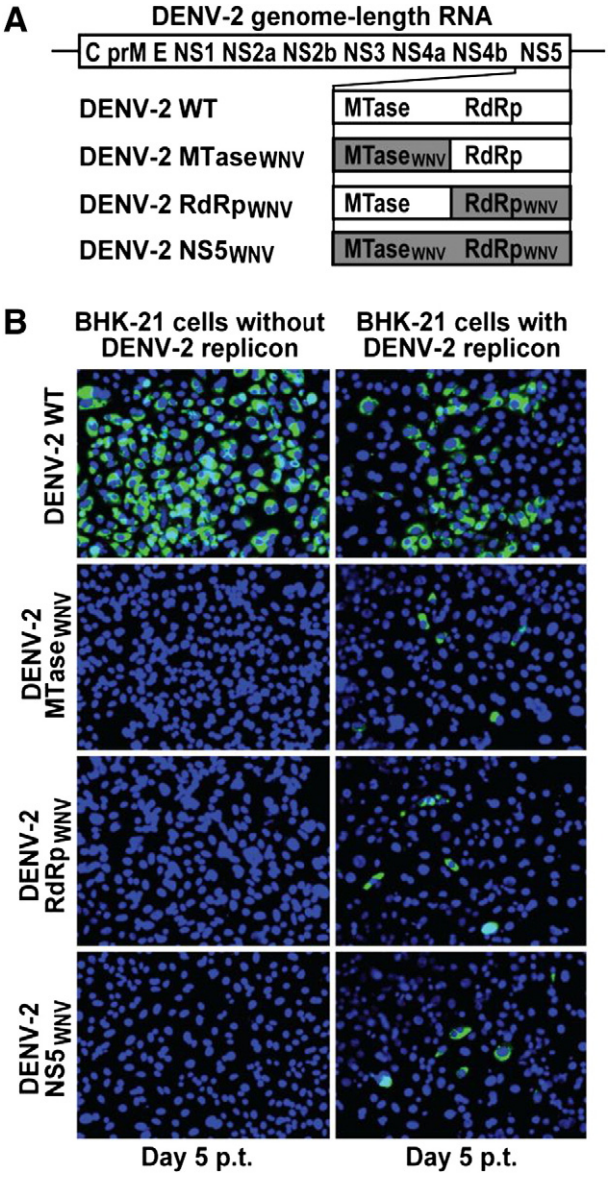

Fig. 7. *trans*-Complementation of chimeric DENVs containing WNV NS5. (A) Three chimeric DENV-2 RNAs containing the WNV MTase domain, RdRp domain, or full-length NS5. The WNV fragments were shaded in grey. (B) IFA analysis. Equal amounts of genome-length RNAs (2 μg) representing DENV-2 WT, DENV-2 MTase$_{WNV}$, DENV-2 RdRp$_{WNV}$, and DENV-2 NS5$_{WNV}$ were transfected into BHK-21 cells with or without a DENV-2 replicon. IFA was performed to detect viral E protein expression (stained in green), and nuclei were counterstained with DAPI in blue.

substrate was used (Egloff et al., 2002). Therefore, caution should be taken when selecting substrates for flavivirus MTase study.

DENV MTase requires distinct viral RNA elements for the two methylation events (Chung et al., 2010). The N-7 methylation requires the first 110 nt of DENV genome, indicating that the 5′-terminal two stem-loops are required for RNA positioning to the enzyme surface during N-7 methylation. It is puzzling why such a complex RNA structure is required for the N-7 activity. In contrast, 2′-O methylation could be efficiently performed with 5′ RNA as short as 25 nt (Supplementary Figure). These results suggest that future effort on RNA-MTase cocrystal structure should use viral RNA, as opposed to various RNA cap analogues or nonviral RNAs. So far, cocrystal structures of MTase in complex with cap analogue have been obtained for several flaviviruses (Assenberg et al., 2007; Bollati et al., 2009; Egloff et al., 2007; Geiss et al., 2009); unfortunately, none of the structures captured the conformation for the N-7 or 2′-O catalysis.

From the structure-based mutagenesis analysis, we summarized that two sets of amino acids on the surface of DENV MTase are required for the N-7 and 2′-O methylations (Fig. 8). Although several residues are important for both methylations, the distribution of the 2′-O critical residues (Fig. 8C) is more spread out than that of the N-7 critical residues (Fig. 8B). The overall mutagenesis results are similar between the WNV MTase and the DENV MTase (Fig. 8A), suggesting a common mechanism for flavivirus MTase in cap methylations. These results support the molecular repositioning model for flavivirus MTase (Zhou et al., 2007). For N-7 methylation, guanine N-7 of the substrate GpppA-RNA is positioned to the methyl group of SAM to generate m^{7}GpppA-RNA. For 2′-O methylation, the m^{7}G moiety of m^{7}GpppA-RNA is bound to the GTP-binding pocket so as to register the 2′-OH of the adenosine with SAM, resulting in m^{7}GpppAm-RNA; alternatively, the G moiety of GpppA-RNA binds to the GTP pocket to register the 2′-OH of the adenosine with SAM, generating GpppAm-RNA. In agreement with the activity results, we found that cap analogue m^{7}GpppA binds to the GTP pocket with a higher affinity than the GpppA (Lim et al., unpublished results), partially explaining the observation that the m^{7}GpppA-RNA is a better substrate than the GpppA-RNA for 2′-O methylation.

To further examine the importance of cap methylations for viral replication, we performed mutagenesis using an infectious cDNA clone of DENV-1 (Fig. 5). A mutation (E217A) that completely knocked out 2′-O methylation attenuated DENV replication, whereas a mutation (D146A) that abolished both methylations was lethal for viral replication. Furthermore, a mutation (E149A) that abolished N-7 methylation but retained 49% of the 2′-O methylation activity yielded replicating virus; however, sequencing of the recovered virus showed reversion of the engineered mutation (data not shown). These results suggest, that N-7 methylation, but not 2′-O methylation, is essential for DENV replication. In agreement with our results, Kroschewski et al. (2008) recently showed that DENV defective in cap methylation is attenuated in viral replication. Remarkably, we found that the replication defect of D146A mutant could be rescued by *trans* complementation in replicon-containing cells (Fig. 6). To our knowledge, this is the first study to show successful *trans* complementation for defective MTase in flavivirus. Such *trans* complementation was unsuccessful for MTase (either point mutation or truncation) in WNV (Ray et al., 2006) and Kunjin virus (Khromykh et al., 1998; Khromykh et al., 1999). Furthermore, we demonstrated that chimeric DENVs containing the WNV NS5 (methyltransferase and/or RdRp domains) were nonreplicative, but the replication defects could also be rescued through *trans* complementation (Fig. 7). Collectively, the results suggest a difference in replication complexes among different members of flaviviruses.

In summary, the current study has extended and strengthened the previous results obtained with the WNV MTase to DENV. The similarity between the WNV and DENV results indicates that flavivirus MTase share a common mechanism in methylating viral RNA cap through a molecular repositioning model. Unlike WNV, the replication defect caused by the DENV MTase mutation could be rescued by *trans* complementation with the WT DENV replicon, suggesting a difference in the capping machinery among different flaviviruses. Between the two methylation activities, the N-7 methylation, rather than the 2′-O methylation, could be targeted for potential anti-flavivirus drug discovery.

Materials and methods

Cloning, expression, and purification of wild-type (WT) and mutant MTases of DENV-4

DNA fragment representing the N-terminal 272 amino acids of DENV-4 NS5 (MTase domain) was RT–PCR amplified from DENV-4 genomic RNA (strain MY-22713) using reverse primer 1 and forward primer 2. The RT–PCR product was cloned into expression vector

pGEX4T1 (GE Healthcare) at *Bam*HI and *Xho*I sites, resulting in plasmid pGEX4T1-DENV-4 MTase-272. Mutagenesis of MTase was performed using standard overlap PCR. The complete sequence of each mutant MTase was validated by DNA sequencing.

A

Mutated sites	N-7 activity		2′-O activity	
	DENV-4	WNV	DENV-4	WNV
K-D-K-E motif				
K61A	34	70 [a]	0	0 [a]
D146A	0	0 [a]	0	0 [a]
K181(182)A	16	42 [a]	6	0 [a]
E217(218)A	59	76 [a]	0	0 [a]
SAM-site				
K105A	52	33 [b]	61	70 [b]
H110A	18	10 [b]	58	65 [b]
D131A	17	79 [b]	13	3 [b]
I147A	54	92 [b]	15	5 [b]
GTP-site				
K14 (13) A	67	77 [b]	2	7 [b]
N18 (17) A	100	100 [b]	70	52 [b]
F25 (24) A	15	15 [b]	4	33 [b]
K29 (R28) A	53	96 [b]	15	46 [b]
S150A	100	80 [b]	55	62 [b]
RNA-site				
E35A	52	71 [b]	2	10 [b]
R84A	5	5 [b]	62	100 [b]
W87A	49	11 [b]	4	7 [b]
E149A	0	3 [b]	49	68 [b]

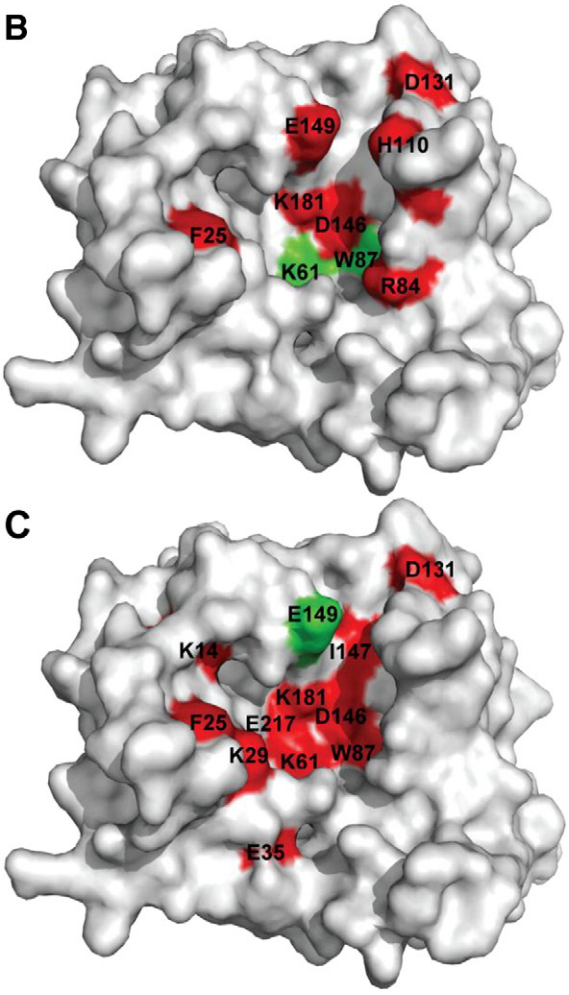

Table 1
Primer sequences.[a]

Primer	Sequence (5′→3′)
1	GCCGCCTCGAGTTATGGTTTTTCTGTTTC[b]
2	ATCAGGATCCGGAACTGGGACCACAGGAGA[c]
3	TAGCACCATCCGTAAGGGTC
4	CAG*TAATACGACTCACTATTA*GTTGTTAGTCTGTGTGGAC[d]
5	TGTCGGTCCACACAGACTAAC
6	GAACTGTCCTTGTCGGTCCAC
7	ACTGTTAGAACTGTGTTAAG
8	TGGTTCATTTTTCCAGAGATC
9	GGTGGTCTAACCACCTTTTTTC
10	AAAGTCCGGTTGAGAATCTCTTCACC
11	AACCCAGTACATGGCATGAGTGGAGTTTC[e]
12	AAAAGGCCTTTCCACAGAGCA
13	AACTCCACTCATGCCATGTACTGGGTTTC[e]
14	CGACGCGTGTCAACTTTCTC
15	AAACGTTCCGTSGCACTGGC
16	GTTTGTGGACRAGCCATGATT

[a] Annotations and usage of the primers are described in Materials and methods.
[b] An *Xho*I site for cloning of MTase is underlined.
[c] A *Bam*HI site for cloning of MTase is underlined.
[d] The italicized sequence represents a bacteriophage T7 class II φ2.5 promoter that was used to synthesize the ATP-initiated RNA (underlined). Three extra nucleotides ("CAG") were added to the 5′ end of the promoter sequence to facilitate efficient transcription.
[e] The mutated nucleoside for D146A substitution are underlined.

All recombinant MTases were fused with an N-terminally GST, expressed in BL21 cells (Novagen), and purified through a GSTPrep™ FF 16/10 column (GE Healthcare). Briefly, *Escherichia coli* BL21 cells bearing the expression plasmid were grown at 37 °C to 0.6~0.8 absorbance optical density at 600 nm (OD_{600}), induced with 0.4 mM isopropyl-β-D-thiogalactopyranoside (IPTG) at 16 °C for 18 h, and harvested by centrifugation. Cell pellets were resuspended and sonicated in a lysis buffer (50 mM Tris–HCl, pH 7.5, 800 mM NaCl, and 5% glycerol) plus 2 mM β-mercaptoethanol. After centrifugation, the lysate supernatant was loaded to a GSTPrep™ FF 16/10 column; the elution containing the recombinant protein was cleaved by thrombin at 4 °C for 16 h; and the cleaved GST was removed from the MTase through the GST column. The proteins (>90% purity) were then concentrated using Amicon ultracel-10 k centrifugal filter (Millipore), quantified by Nanodrop-1000, and verified by sodium dodecyl sulfate–polyacrylamide gel electrophoresis (SDS–PAGE).

Preparation of RNA substrates

A PCR template-mediated *in vitro* transcription was used to prepare RNAs representing various 5′-terminal lengths of DENV genome. All PCRs used the same cDNA template representing the first 211 nucleotides of DENV-4 genome. The 211-bp cDNA template was prepared by reverse transcription (RT) using genomic RNA of DENV-4 (strain MY-22713), reverse primer 3, and SuperScript™ III Reverse Transcriptase (Invitrogen). The RT reaction was performed according the manufacturer's protocol. Two microliters of the RT reaction mixture was used as a template for PCR amplification.

RNAs representing the first 25, 35, 70, 110, 134, and 211 nucleotides of DENV-4 genome were *in vitro* transcribed from corresponding PCR products. The PCR products were generated by using the 211-bp cDNA (described above) as a template, a common

Fig. 8. Comparison of mutagenesis results from DENV and WNV MTases. (A) Summary of mutagenesis data from DENV and WNV MTases. The DENV MTase data are from the current study. The WNV MTase results are derived from Zhou et al. (2007) and Dong et al. (2008b), as indicated by "a" and "b," respectively. Residues important for N-7 (B) and 2′-O methylations (C) are presented on the surface of DENV-2 MTase (PDB code: 1L9K; Egloff et al., 2002). Residues whose mutations led to reductions in activity to <20% of the WT level are in red; residues whose mutations led to reductions in activity to 20–50% of the WT activity are in green. The images were prepared using PyMOL.

forward primer 4 and a corresponding reverse primer 5, 6, 7, 8, 9, or 10, respectively (Table 1). Primer 4 contained a modified bacteriophage T7 class II φ2.5 promoter (italicized in Table 1; Coleman et al., 2004) to facilitate synthesis of ATP initiated RNA using MEGAshortscript kit (Applied Biosystems). *In vitro* synthesized RNAs were capped using [α-^{33}P] GTP (PerkinElmer) and a vaccinia virus capping enzyme (Epicentre) in the presence or absence of cold SAM according to the manufacturer's instructions. The resulting 5′-labeled m^{7}G*pppA and G*pppA-RNA (the asterisk indicates that the following phosphate is ^{33}P-labeled) were used as substrates for N-7 and 2′-O methylations, respectively. For the removal of unincorporated [α-^{33}P] GTP, the capping reactions were passed through two G-25 size columns (GE Healthcare), extracted with phenol–chloroform, and precipitated with ethanol.

N-7 and 2′-O methylation assays

The N-7 methylation was performed in a 20-μl reaction containing 50 mM Bis–Tris [pH 6.0], 50 mM NaCl, 2 mM dithiothreitol [DTT], ~2×10^5 cpm G*pppA-RNA, 50 μM SAM, and 0.2 μM MTase at 22 °C for 5 min. 2′-O methylation was performed in a 20-μl reaction containing 50 mM Tris–HCl [pH 9.0], 1 mM $MgCl_2$, 2 mM DTT, ~2×10^5 cpm m^{7}G*pppA-RNA, 50 μM SAM, and 0.2 μM MTase at 22 °C for 1 h. All methylation reactions were digested with nuclease P1 in 20 mM Tris–HCl [pH 7.5] buffer at 37°C overnight and analyzed on polyethyleneimine cellulose thin-layer chromatography (TLC) plates (JT Baker) using a solvent of 0.65 M LiCl. The radioactive cap structures on TLC plates were quantified by a PhosphorImager.

E149A MTase-mediated 2′-O methylation assay

Two substrates, m^{7}G*pppA-RNA and G*pppA-RNA (211 nt), were incubated with E149A MTase in the 2′-O buffer (see above) at 22 °C for various time periods. The reactions were then treated with nuclease P1 at 37 °C for overnight. As controls, cap methylation with ScriptCap™ 2′-O-Methyltransfease (VP39; Epicentre) was performed in a 20-μl reaction containing 50 mM Tris–HCl (pH 8.0), 6 mM KCl, 1.25 mM $MgCl_2$, 25 μM SAM, 4 pmol m^{7}G*pppA-RNA or G*pppA-RNA, and 50 ng VP39; the reaction was incubated at 37 °C for 1 h. The reaction mixtures were separated on a 20% polyacrylamide gel (16×35 cm^2) with 8 M urea. The bands representing different cap structures (G*pppA, G*pppAm, m^{7}G*pppA, and m^{7}G*pppAm) were quantified using a PhosphorImager.

Construction of mutant full-length cDNA of DENV-1

A full-length cDNA clone of DENV-1 (Western Pacific 74 strain; GenBank accession U88535) was constructed using a low-copy number plasmid pACYC177 (New England Biolabs). The details of the cDNA construction will be described elsewhere. The pACYA177-DENV-1 plasmid was used to engineer the E216A mutation of the K-D-K-E motif. Overlapping PCRs, with one PCR prepared with primers 11 and 12 and another PCR prepared with primers 13 and 14, were fused together. The resulting PCR product, containing the E216A substitution, was inserted into the WT pACYA177-DENV-1 plasmid using the *StuI* and *MluI* sites. A similar overlapping PCR approach was used to prepare cDNA clones for chimeric DENVs containing the WNV NS5 (MTase and/or RdRp). All cDNA plasmids were verified by DNA sequencing.

In vitro transcription, RNA transfection, and immunofluorescence assay (IFA)

The assay protocols used were described previously (Shi et al., 2002). Briefly, RNAs were transcribed from full-length cDNA plasmids and then electroporated into BHK-21 cells. Viral protein synthesis in transfected cells was monitored by IFA with DEN-immune mouse 4G2 (American Type Culture Collection) and anti-mouse immunoglobulin G conjugated with FITC as the primary and secondary antibodies, respectively.

Plaque assay and viral genome sequencing

Viral titers of culture fluids from BHK-21 cells at day 5 post-transfection (p.t.) were quantified through a single-layer plaque assay. The stabilities of mutant viruses were examined by continuous passaging of the viruses in Vero cells for four passages (3 days per passage), followed by comparison of the plaque morphologies of the passaged and unpassaged viruses. For each recovered virus, viral RNA was extracted with an RNeasy kit (Qiagen), the NS5 gene was amplified by using One-Step RT–PCR kit (Invitrogen), and the complete MTase domain of the PCR product was sequenced.

Trans complementation assay

Equal amounts of WT and D146A genome-length RNAs (2 μg) were transfected into naive BHK-21 cells or BHK-21 cells containing a DENV replicon (Puig-Basagoiti et al., 2006). On day 4 post-transfection, total RNAs were extracted from cells and culture supernatants using an RNeasy kit. The extracted RNAs were subjected to RT–PCR amplification following the manufacturer's protocol (Invitrogen). Forward primers 15 and reverse primer 16 (Table 1), located in the prM and E genes, respectively, were used to amplify an 862-bp fragment from nucleotide position 704 to 1565.

Acknowledgment

We thank colleagues at Novartis Institute for Tropical Diseases for helpful discussions during the course of this work.

Appendix A. Supplementary data

Supplementary data associated with this article can be found, in the online version, at doi:10.1016/j.virol.2010.06.039.

References

Assenberg, R., Ren, J., Verma, A., Walter, T.S., Alderton, David, Hurrelbrink, R.J., Fuller, S.D., Bressanelli, S., Owens, R.J., Stuart, D.I., Grimes, J.M., 2007. Crystal structure of the Murray Valley encephalitis virus NS5 methyltransferase domain in complex with cap analogues. J. Gen. Virol. 88, 2228–2236.

Bollati, M., Milani, M., Mastrangelo, E., Ricagno, S., Tedeschi, G., Nonnis, S., Decroly, E., Selisko, B., de Lamballerie, X., Coutard, B., Canard, B., Bolognesi, M., 2009. Recognition of RNA cap in the Wesselsbron virus NS5 methyltransferase domain: implications for RNA-capping mechanisms in flavivirus. J. Mol. Biol. 385 (1), 140–152.

Chung, K.Y., Dong, H., Chao, A.T., Shi, P.Y., Lescar, J., Lim, S.P., 2010. Higher catalytic efficiency of N-7-methylation is responsible for processive N-7 and 2′-O methyltransferase activity in dengue virus. Virology 402 (1), 52–60.

Cleaves, G.R., Dubin, D.T., 1979. Methylation status of intracellular dengue type 2 40S RNA. Virology 96, 159–165.

Coleman, T.M., Wang, G., Huang, F., 2004. Superior 5′ homogeneity of RNA from ATP-initiated transcription under the T7 phi 2.5 promoter. Nucleic Acids Res. 32 (1), e14.

Dong, H., Ray, D., Ren, S., Zhang, B., Puig-Basagoiti, F., Takagi, Y., Ho, C., Li, H., Shi, P.Y., 2007. Distinct RNA elements confer specificity to flavivirus RNA cap methylation events. J. Virol. 81 (9), 4412–4421.

Dong, H., Ren, S., Li, H., Shi, P.Y., 2008a. Separate molecules of West Nile virus methyltransferase can independently catalyze the N7 and 2′-O methylations of viral RNA cap. Virology 377 (1), 1–6.

Dong, H., Ren, S., Zhang, B., Zhou, Y., Puig-Basagoiti, F., Li, H., Shi, P.Y., 2008b. West Nile virus methyltransferase catalyzes two methylations of the viral RNA cap through a substrate-repositioning mechanism. J. Virol. 82 (9), 4295–4307.

Dong, H., Zhang, B., Shi, P.Y., 2008c. Flavivirus methyltransferase: a novel antiviral target. Antivir. Res. 80 (1), 1–10.

Egloff, M.P., Benarroch, D., Selisko, B., Romette, J.L., Canard, B., 2002. An RNA cap (nucleoside-2′-O-)-methyltransferase in the flavivirus RNA polymerase NS5: crystal structure and functional characterization. EMBO J. 21 (11), 2757–2768.

Egloff, M.P., Decroly, E., Malet, H., Selisko, B., Benarroch, D., Ferron, F., Canard, B., 2007. Structural and functional analysis of methylation and 5′-RNA sequence requirements of short capped RNAs by the methyltransferase domain of dengue virus NS5. J. Mol. Biol. 372, 723–736.

Furuichi, Y., Shatkin, A.J., 2000. Viral and cellular mRNA capping: past and prospects. Adv. Virus Res. 55, 135–184.
Geiss, B.J., Thompson, A.A., Andrews, A.J., Sons, R.L., Gari, H.H., Keenan, S.M., Peersen, O.B., 2009. Analysis of flavivirus NS5 methyltransferase cap binding. J. Mol. Biol. 385 (5), 1643–1654.
Gubler, D., Kuno, G., Markoff, L., 2007. Flaviviruses, In: Knipe, D.M., Howley, P.M. (Eds.), 5th. Fields virology, vol. 1. Lippincott William & Wilkins, Philadelphia, PA, pp. 1153–1253.
Hager, J., Staker, B.L., Bugl, H., Jakob, U., 2002. Active site in RrmJ, a heat shock-induced methyltransferase. J. Biol. Chem. 277 (44), 41978–41986.
Hodel, A.E., Gershon, P.D., Quiocho, F.A., 1998. Structural basis for sequence-nonspecific recognition of 5′-capped mRNA by a cap-modifying enzyme. Mol. Cell 1 (3), 443–447.
Hodel, A.E., Gershon, P.D., Shi, X., Quiocho, F.A., 1996. The 1.85 A structure of vaccinia protein VP39: a bifunctional enzyme that participates in the modification of both mRNA ends. Cell 85 (2), 247–256.
Issur, M., Geiss, B.J., Bougie, I., Picard-Jean, F., Despins, S., Mayette, J., Hobdey, S.E., Bisaillon, M., 2009. The flavivirus NS5 protein is a true RNA guanylyltransferase that catalyzes a two-step reaction to form the RNA cap structure. Rna 15 (12), 2340–2350.
Khromykh, A., Kenney, M., Westaway, E., 1998. *trans*-Complementation of flavivirus RNA polymerase gene NS5 by using Kunjin virus replicon-expressing BHK cells. J. Virol. 72 (9), 7270–7279.
Khromykh, A.A., Sedlak, P.L., Westaway, E.G., 1999. *trans*-Complementation analysis of the flavivirus Kunjin ns5 gene reveals an essential role for translation of its N-terminal half in RNA replication. J. Virol. 73 (11), 9247–9255.
Kroschewski, H., Lim, S.P., Butcher, R.E., Yap, T.L., Lescar, J., Wright, P.J., Vasudevan, S.G., Davidson, A.D., 2008. Mutagenesis of the dengue virus type 2 NS5 methyltransferase domain. J. Biol. Chem. 283 (28), 19410–19421.
Li, H., Clum, S., You, S., Ebner, K.E., Padmanabhan, R., 1999. The serine protease and RNA-stimulated nucleoside triphosphatase and RNA helicase functional domains of dengue virus type 2 NS3 converge within a region of 20 amino acids. J. Virol. 73 (4), 3108–3116.
Lim, S.P., Wen, D., Yap, T.L., Yan, C.K., Lescar, J., Vasudevan, S.G., 2008. A scintillation proximity assay for dengue virus NS5 2′-O-methyltransferase—kinetic and inhibition analyses. Antivir. Res. 80 (3), 360–369.
Lindenbach, B.D., Thiel, H.-J., Rice, C.M., 2007. *Flaviviridae*: the virus and their replication, In: Knipe, D.M., Howley, P.M. (Eds.), 5th. Fields Virology, vol. 1. Lippincott William & Wilkins, Philadelphia, PA, pp. 1101–1152.
Puig-Basagoiti, F., Tilgner, M., Forshey, B., Philpott, S., Espina, N., Wentworth, Goebel, S., Masters, P.S., Falgout, B., Ren, P., Ferguson, Shi, P.Y., 2006. Triaryl pyrazoline compound inhibits flavivirus RNA replication. Antimicrob. Agents Chemother. 50 (4), 1320–1329.
Ray, D., Shah, A., Tilgner, M., Guo, Y., Zhao, Y., Dong, H., Deas, T., Zhou, Y., Li, H., Shi, P.-Y., 2006. West Nile virus 5′-cap structure is formed by sequential guanine N-7 and ribose 2′-O methylations by nonstructural protein 5. J. Virol. 80 (17), 8362–8370.
Selisko, B., Peyrane, F.F., Canard, B., Alvarez, K., Decroly, E., 2010. Biochemical characterization of the (nucleoside-2′O)-methyltransferase activity of dengue virus protein NS5 using purified capped RNA oligonucleotides (7Me)GpppAC(n) and GpppAC(n). J. Gen. Virol. 91 (Pt 1), 112–121.
Shi, P.Y., Tilgner, M., Lo, M.K., Kent, K.A., Bernard, K.A., 2002. Infectious cDNA clone of the epidemic West Nile virus from New York City. J. Virol. 76 (12), 5847–5856.
Shuman, S., 2001. Structure, mechanism, and evolution of the mRNA capping apparatus. Prog. Nucleic Acid Res. Mol. Biol. 66, 1–40.
Wengler, G., 1981. Terminal sequences of the genome and replicative-form RNA of the flavivirus West Nile virus: absence of poly(A) and possible role in RNA replication. Virology 113 (2), 544–555.
Wengler, G., Wengler, G., 1991. The carboxy-terminal part of the NS 3 protein of the West Nile flavivirus can be isolated as a soluble protein after proteolytic cleavage and represents an RNA-stimulated NTPase. Virology 184 (2), 707–715.
Zhang, B., Dong, H., Zhou, Y., Shi, P.Y., 2008. Genetic interactions among the West Nile virus methyltransferase, the RNA-dependent RNA polymerase, and the 5′ stem-loop of genomic RNA. J. Virol. 82 (14), 7047–7058.
Zhang, X., Tamaru, H., Khan, S.I., Horton, J.R., Keefe, L.J., Selker, E.U., Cheng, X., 2002. Structure of the Neurospora SET domain protein DIM-5, a histone H3 lysine methyltransferase. Cell 111 (1), 117–127.
Zhou, Y., Ray, D., Zhao, Y., Dong, H., Ren, S., Li, Z., Guo, Y., Bernard, K., Shi, P.-Y., Li, H., 2007. Structure and function of flavivirus NS5 methyltransferase. J. Virol. 81 (8), 3891–3903.
Zou, G., Zhang, B., Lim, P.Y., Yuan, Z., Bernard, K.A., Shi, P.Y., 2009. Exclusion of West Nile virus superinfection through RNA replication. J. Virol. 83 (22), 11765–11776.